

## Measurements of $J/\psi$ production in Pb–Pb collisions at $\sqrt{s_{NN}} = 5.02$ TeV with ALICE

---

Pengzhong Lu<sup>a,b,\*</sup> for the ALICE Collaboration

<sup>a</sup>*Department of Modern Physics, University of Science and Technology of China,  
Jinzhai 96, Hefei, China*

<sup>b</sup>*GSI Helmholtzzentrum für Schwerionenforschung GmbH,  
Planckstraße 1, Darmstadt, Germany*

*E-mail:* [pengzhong.lu@cern.ch](mailto:pengzhong.lu@cern.ch)

In these proceedings, the latest charmonium measurements carried out by the ALICE collaboration at midrapidity and forward rapidity in Pb–Pb collisions at  $\sqrt{s_{NN}} = 5.02$  TeV, are presented. These include the recently published inclusive  $J/\psi$  yield and nuclear modification factor ( $R_{AA}$ ) at midrapidity and forward rapidity, as well as preliminary measurements of prompt and non-prompt  $J/\psi$   $R_{AA}$  at midrapidity. The measurements of the non-prompt  $J/\psi$  fraction extend down to transverse momentum  $p_T = 1.5$  GeV/ $c$  with a significantly improved precision compared to previous published results. Results are compared with model calculations.

*HardProbes2023  
26-31 March 2023  
Aschaffenburg, Germany*

---

\*Speaker

## 1. Introduction

Heavy quarks, such as charm and beauty, play a crucial role in studying quantum chromodynamics (QCD) in high-energy hadronic collisions. They provide insights into various aspects of QCD, ranging from production mechanisms in proton–proton collisions (pp) to the properties of the hot and dense quark-gluon plasma (QGP) formed in nucleus–nucleus (AA) collisions.

In pp collisions, perturbative QCD calculations can accurately describe the partonic hard scattering processes involving heavy quarks down to low transverse momentum ( $p_T$ ) [1]. The formation of quarkonia, involves non-perturbative effects due to long distances and soft momentum scales. Therefore, studying quarkonium production provides valuable insights into both perturbative and non-perturbative aspects of QCD [2].

In AA collisions, open and hidden heavy quark hadron production serves as a sensitive probe of the QGP. Heavy-quark production occurs via hard scattering processes, at times scale that are typically shorter than the QGP thermalization time. QGP formation modifies the potential between heavy quarks, leading to color screening [3] and dynamical dissociation [4]. At high centre-of-mass energies, the (re)combination mechanism could play an important role in the case of charmonium either during the deconfined [5] or hadronization [6] stages. Additionally, heavy quarks experience energy loss as they propagate in the QGP, which depends on the medium properties such as energy density and temperature. Therefore, the study of the production of non-prompt J/ψ mesons, originating from beauty hadron decays, provides valuable insights into energy loss mechanisms for beauty quarks, as well as the transport properties of the QGP [2].

The inclusive J/ψ production has been extensively studied in heavy-ion collisions. Measurements at LHC energies show less suppression compared to results from RHIC, particularly at low  $p_T$  [7, 8]. This was the first evidence for charmonium (re)combination at LHC energies. These proceedings present the inclusive J/ψ production, covering a broad  $p_T$  range at midrapidity ( $|y| < 0.9$ ) and forward rapidity ( $2.5 < y < 4.0$ ), utilizing the full sample of Pb–Pb collisions at  $\sqrt{s_{NN}} = 5.02$  TeV collected by the ALICE detector during the LHC Run 2. In addition, contributions from prompt and non-prompt J/ψ production are disentangled at midrapidity and results are discussed together with model comparisons.

## 2. Inclusive J/ψ yields and nuclear modification factor

The inclusive J/ψ  $p_T$ -differential yields are obtained for different centrality intervals in Pb–Pb collisions at  $\sqrt{s_{NN}} = 5.02$  TeV at midrapidity and forward rapidity [9]. Figure 1 shows the J/ψ yields in the 0–10% and 0–20% centrality classes for midrapidity (left) and forward rapidity (right), respectively. Statistical uncertainties are represented by vertical error bars, while systematic uncertainties are indicated by open boxes. The results are compared to the statistical hadronization model (SHMc) [6] and two microscopic transport models [10, 11]. The transport models describe the  $p_T$ -differential yields well in central collisions both at midrapidity and forward rapidity. The SHMc calculations, incorporating a freezeout parameterization inspired by hydrodynamics, exhibit good agreement with the data in the low- $p_T$  region but underestimate the measurements at higher  $p_T$ .

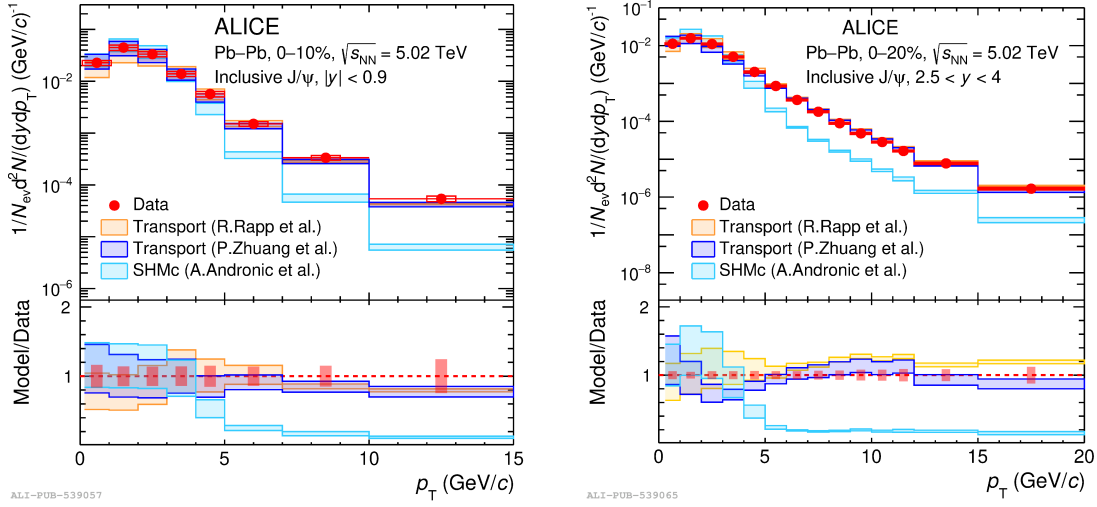


**Figure 1:**  $J/\psi$   $p_T$ -differential production yields in Pb–Pb collisions at  $\sqrt{s_{NN}} = 5.02$  TeV at midrapidity in the 0–10% centrality interval (left panel) and at forward rapidity in the 0–20% centrality interval (right panel).

The nuclear modification factor ( $R_{AA}$ ) is defined as the ratio of yields in AA collisions with respect to pp collisions scaled by the number of binary nucleon–nucleon collisions. Figure 2 (left panel) presents the  $p_T$ -integrated  $J/\psi$   $R_{AA}$  as a function of the average number of participant nucleons,  $\langle N_{part} \rangle$ , in Pb–Pb collisions at  $\sqrt{s_{NN}} = 5.02$  TeV [9]. The data are compared with the previously published results at forward rapidity [12]. Low- $p_T$   $J/\psi$  contributions from photoproduction processes are excluded, with a selection of  $p_T > 0.15$  GeV/c and  $p_T > 0.3$  GeV/c at midrapidity and forward rapidity, respectively.

The  $R_{AA}$  values are close to unity in most peripheral collisions, indicating no significant medium modification, while a suppression of  $J/\psi$  production is observed in semi-central (and central at forward rapidity) Pb–Pb collisions. Furthermore, the  $R_{AA}$  at midrapidity is higher than that at forward rapidity in central and semicentral collisions, reflecting the higher contribution from (re)generation, due to the larger  $c\bar{c}$  density at midrapidity.

In the right panel of Figure 2, the  $R_{AA}$  is shown as a function of  $\langle N_{part} \rangle$  at midrapidity, along with calculations from SHMc [6] and two transport models [10, 11]. Within the uncertainties of the models, all three predictions are consistent with the data. Notably, the data lie on the upper edge of the transport model calculations, while they agree well with the central values from the SHMc calculations for semicentral and central collisions.

Figure 3 displays the  $p_T$ -differential  $R_{AA}$  measurements for the 0–10% centrality interval at midrapidity (left) and 0–20% at forward rapidity (right) [9], along with model calculations. The SHMc model agrees well with the data at low  $p_T$  in both rapidity ranges. However, for  $p_T > 5$  GeV/c, it underestimates the  $R_{AA}$  in all centrality intervals and rapidities. In contrast, the two transport models show better quantitative agreement with the data. They provide a good description of the  $R_{AA}$  at both low and high  $p_T$ . Moreover, energy-loss calculations from Ref. [13], available for  $p_T > 10$  GeV/c, agree well with the measurements in all centrality ranges. These calculations suggest that energy loss is a dominant mechanism in this kinematic regime, consistently with measurements of other charm hadrons at LHC energies.

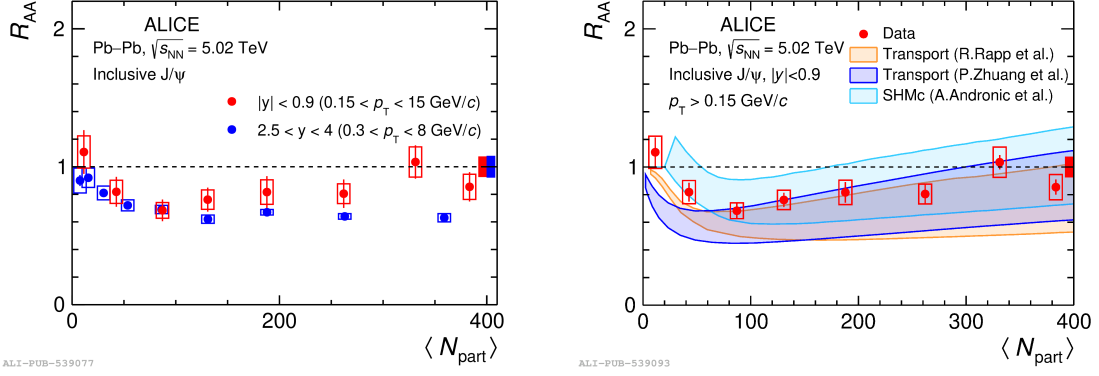


**Figure 2:** Inclusive  $J/\psi$   $R_{AA}$  at midrapidity and forward rapidity as a function of  $\langle N_{part} \rangle$  (left panel). Inclusive  $J/\psi$   $R_{AA}$  at midrapidity as a function of  $\langle N_{part} \rangle$  [9, 12] compared to model calculations [6, 10, 11] (right panel).

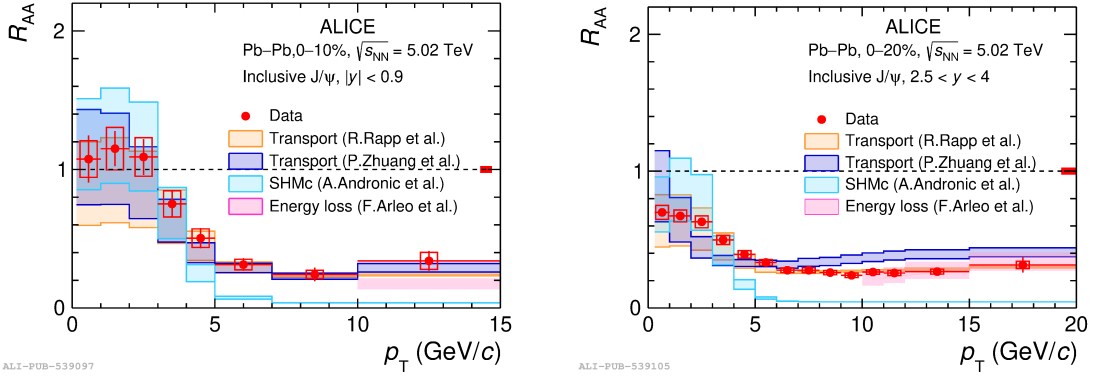


**Figure 3:** Inclusive  $J/\psi$   $R_{AA}$   $p_T$  dependence at midrapidity in the 0–10% centrality interval (left) and forward rapidity in 0–20% centrality interval (right) [9]. The results are compared with model calculations from [6, 10, 11, 13].

### 3. Prompt and non-prompt $J/\psi$ nuclear modification factors

The nuclear modification factor,  $R_{AA}$ , of prompt and non-prompt  $J/\psi$  within a given  $p_T$  range are determined as:

$$R_{AA}^{\text{Prompt } J/\psi} = \frac{1 - f_B^{\text{Pb-Pb}}}{1 - f_B^{\text{PP}}} R_{AA}^{\text{Inclusive } J/\psi}, \quad R_{AA}^{\text{Non-prompt } J/\psi} = \frac{f_B^{\text{Pb-Pb}}}{f_B^{\text{PP}}} R_{AA}^{\text{Inclusive } J/\psi} \quad (1)$$

where  $f_B^{\text{Pb-Pb}}$  and  $f_B^{\text{PP}}$  are the non-prompt  $J/\psi$  fractions and  $R_{AA}^{\text{Inclusive } J/\psi}$  is the inclusive  $J/\psi$   $R_{AA}$  discussed in the previous section.

The results for prompt and non-prompt  $J/\psi$   $R_{AA}$  in the most central collisions (0–10%) are shown in Figures 4a and 4b, and for semicentral collisions (30–50%) in Figures 4c and 4d. In addition, results from the non-prompt  $D^0$  meson in the 0–10% (30–50%) centrality interval are also presented in Figure 4b (Figure 4d) and compared to the non-prompt  $J/\psi$   $R_{AA}$ . The results show a reasonable agreement between non-prompt  $D^0$  [14] and non-prompt  $J/\psi$  production within the uncertainties, despite possible differences originating from different decay kinematics of beauty

hadrons into  $J/\psi$  and  $D^0$ . Additionally, the ALICE results are compared to CMS [15] and ATLAS [16] measurements obtained at higher  $p_T$  for Pb–Pb collisions at the same center-of-mass energy and for similar centrality intervals. ALICE extends these measurements down to  $p_T = 1.5$  GeV/ $c$ .

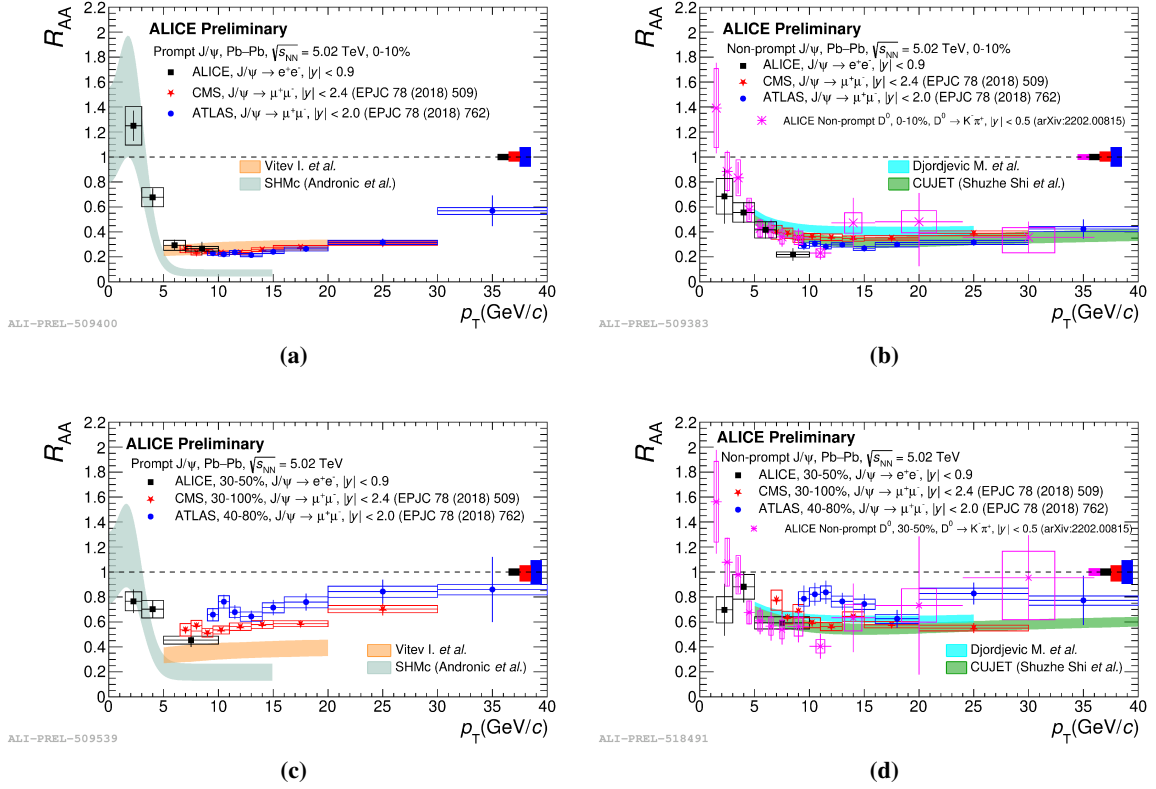


**Figure 4:** Prompt (left  $\rightarrow$  a,c) and non-prompt (right  $\rightarrow$  b,d)  $J/\psi$   $R_{AA}$  as a function of  $p_T$  in the centrality bin 0–10% (top  $\rightarrow$  a,b) and 30–50% (bottom  $\rightarrow$  c,d). The results are compared with model calculations from [6, 17–20].

The prompt  $J/\psi$   $R_{AA}$  exhibits an increasing trend towards low  $p_T$  both in semi-central and central collisions (with a larger increase in central collisions), which is reproduced by the SHMc model calculations [6] for  $p_T < 5$  GeV/ $c$ . The model by Vitev et al. [17, 18] reproduces the prompt  $J/\psi$  suppression for  $p_T > 5$  GeV/ $c$  in central collisions. For non-prompt  $J/\psi$ , a similar trend of strong suppression is observed, as shown in Figures 4b and 4d, at high  $p_T$  as well as an increasing trend towards low  $p_T$  similar to the one of non-prompt  $D^0$ . The results for non-prompt  $J/\psi$  production are consistent at high  $p_T$  with energy-loss models incorporating both collisional and radiative contributions [19, 20].

#### 4. Conclusions

ALICE extends measurements on inclusive  $J/\psi$  production down to zero  $p_T$  and prompt and non-prompt  $J/\psi$  measurements down to  $p_T = 1.5$  GeV/ $c$  in Pb–Pb collisions at  $\sqrt{s_{\text{NN}}} = 5.02$  TeV. Effects of (re)generation in the QGP or at hadronization lead to an increasing trend of the inclusive

and prompt J/ $\psi$   $R_{AA}$  towards central collisions and low  $p_T$ . The suppression factor  $R_{AA}$  for non-prompt  $D^0$  and non-prompt J/ $\psi$  exhibits a similar trend, showing a strong suppression at high  $p_T$  described by collisional and radiative energy loss models.

## Acknowledgment

The author is supported in part by the National Key Research and Development Program of China under grant No. 2018YFE0104900, National Natural Science Foundation of China under grant No. 12061141008 and 12105277, and EU-H2020: 824093-STRONG-WPX-NA7 (10505).

## References

- [1] M. Cacciari *J. Phys. G* **34** (2007) S479 [arXiv:hep-ph/0702211].
- [2] A. Andronic et al. *Eur. Phys. J. C* **76** (2016) 107 [arXiv:1506.03981].
- [3] T. Matsui and H. Satz *Phys. Lett. B* **178** (1986) 416.
- [4] A. Rothkopf *Phys. Rept.* **858** (2020) 1 [arXiv:1912.02253].
- [5] R.L. Thews and M.L. Mangano *Phys. Rev. C* **73** (2006) 014904 [arXiv:nucl-th/0505055].
- [6] A. Andronic et al. *Phys. Lett. B* **797** (2019) 134836 [arXiv:1901.09200].
- [7] STAR collaboration *Phys. Lett. B* **771** (2017) 13 [arXiv:1607.07517].
- [8] ALICE collaboration *JHEP* **07** (2015) 051 [arXiv:1504.07151].
- [9] ALICE collaboration arXiv:2303.13361.
- [10] K. Zhou, N. Xu, Z. Xu and P. Zhuang *Phys. Rev. C* **89** (2014) 054911 [arXiv:1401.5845].
- [11] X. Zhao and R. Rapp *Phys. Lett. B* **664** (2008) 253 [arXiv:0712.2407].
- [12] ALICE collaboration *Phys. Lett. B* **766** (2017) 212 [arXiv:1606.08197].
- [13] F. Arleo *Phys. Rev. Lett.* **119** (2017) 062302 [arXiv:1703.10852].
- [14] ALICE collaboration *JHEP* **12** (2022) 126 [arXiv:2202.00815].
- [15] CMS collaboration *Eur. Phys. J. C* **78** (2018) 509 [arXiv:1712.08959].
- [16] ATLAS collaboration *Eur. Phys. J. C* **78** (2018) 762 [arXiv:1805.04077].
- [17] S. Aronson et al. *Phys. Lett. B* **778** (2018) 384 [arXiv:1709.02372].
- [18] Y. Makris and I. Vitev *JHEP* **10** (2019) 111 [arXiv:1906.04186].
- [19] D. Zigic et al. *Front. in Phys.* **10** (2022) 957019 [arXiv:2110.01544].
- [20] S. Shi, J. Liao and M. Gyulassy *Chinese Physics C* **43** (2019) 044101.